

Supplementary Information

Unveiling the (de-)lithiation mechanism of nano-sized LiMn_2O_4 allows to design a cycling protocol for achieving long-term cycling stability

Juliana B. Falqueto^{1,2*}, Adam H. Clark³, Łukasz Kondracki², Nerilso Bocchi¹, Mario El Kazzi^{2*}

¹ Federal University of São Carlos, Department of Chemistry, C.P. 676, 13560-970 São Carlos - SP, Brazil

² Electrochemistry Laboratory, PSI, CH-5232 Villigen PSI, Switzerland

³ Photon Science Division, PSI, CH-5232 Villigen PSI, Switzerland

* Corresponding author: juliana.bruneli-falqueto@psi.ch, mario.el-kazzi@psi.ch

The following Supplementary Information contains:

- EIS spectra acquired after the 1st discharge at 2.0 V + 5 min of OCP, for electrodes prepared from nano and micron-sized spinel samples.
- Reverse Monte Carlo results of *operando* EXAFS data for nano-sized spinel.
- *Operando* diffraction patterns collected at different cycling states for nano-sized spinel.
- Results of the Rietveld analysis of *operando* XRD patterns: amount of tetragonal phase and I41/amd lattice cell parameters *a* and *c*, tables, and plots of the fits.
- *Operando* XRD to track the evolution of different structures during 1st cycle and 2nd charge of electrode prepared from micron-sized LiMn_2O_4 spinel before and after correction the patterns intensity.
- Specific discharge capacity obtained for the cathodes cycled in a voltage range of 2.0 to 4.3 V using the cycling protocol proposed.

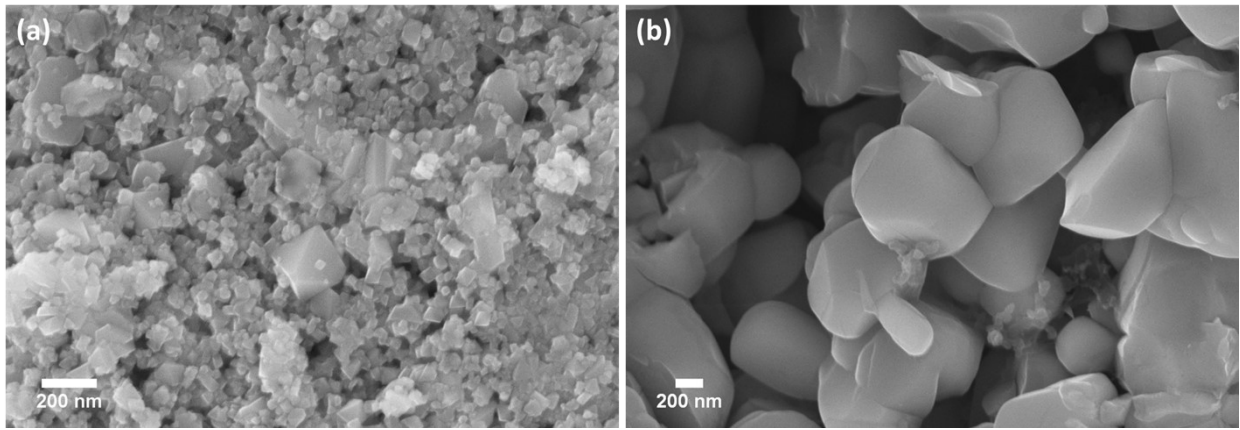


Figure S. 1. SEM images of (a) nano and (b) micron-sized LMO spinel cathodes before cycling.

Figure S.2 shows the EIS spectra, which monitor the internal resistance to charge transfer of the spinel active materials after the 1st discharge at 2.0 V and 5 min of OCP. The size of the depressed semicircles in the Nyquist plots represent the charge transfer resistance (R_{CT}) contribution from the cathode–electrolyte interface and the high-frequency x-intercept represent the Ohmic resistance of the electrolyte. In the discharging state, after the electrodes completing 5 min of OCP rest, were observed a smaller semicircle for the nano-sized spinel electrode than for micron-sized. This result indicates that the nanoparticles present a lower R_{CT} than the micron particles at this potential, which corroborates with the results from *operando* XAS measurements. Micron-sized spinel, in comparison with the nano-sized, presents a bigger hindrance to reduce the Mn^{4+} to Mn^{3+} , what indicates a higher resistance to transfer charge and, consequently, Li ion insertion into the structure of the cathode is compromised.

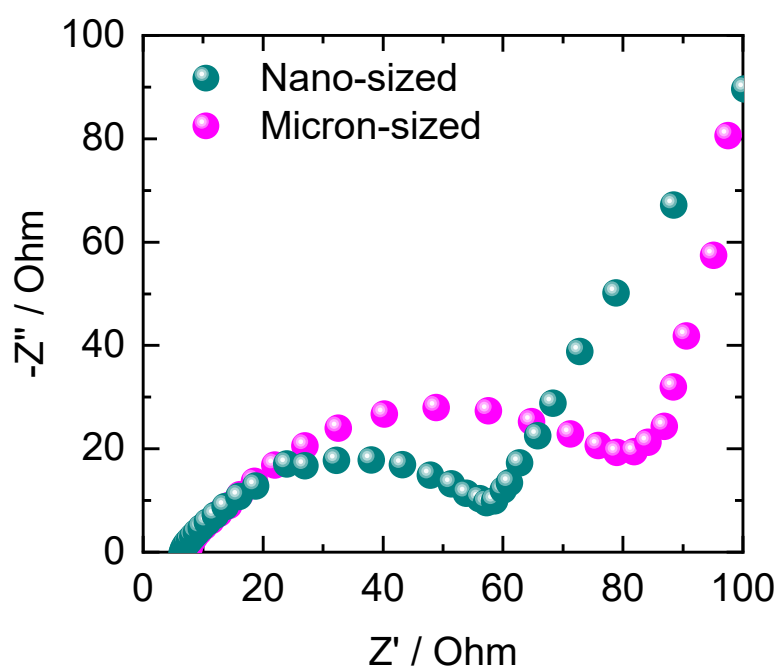


Figure S.2. EIS spectra acquired in after the 1st discharge at 2.0 V + 5 min of OCP , for electrodes prepared from nano and micron-sized spinel samples.

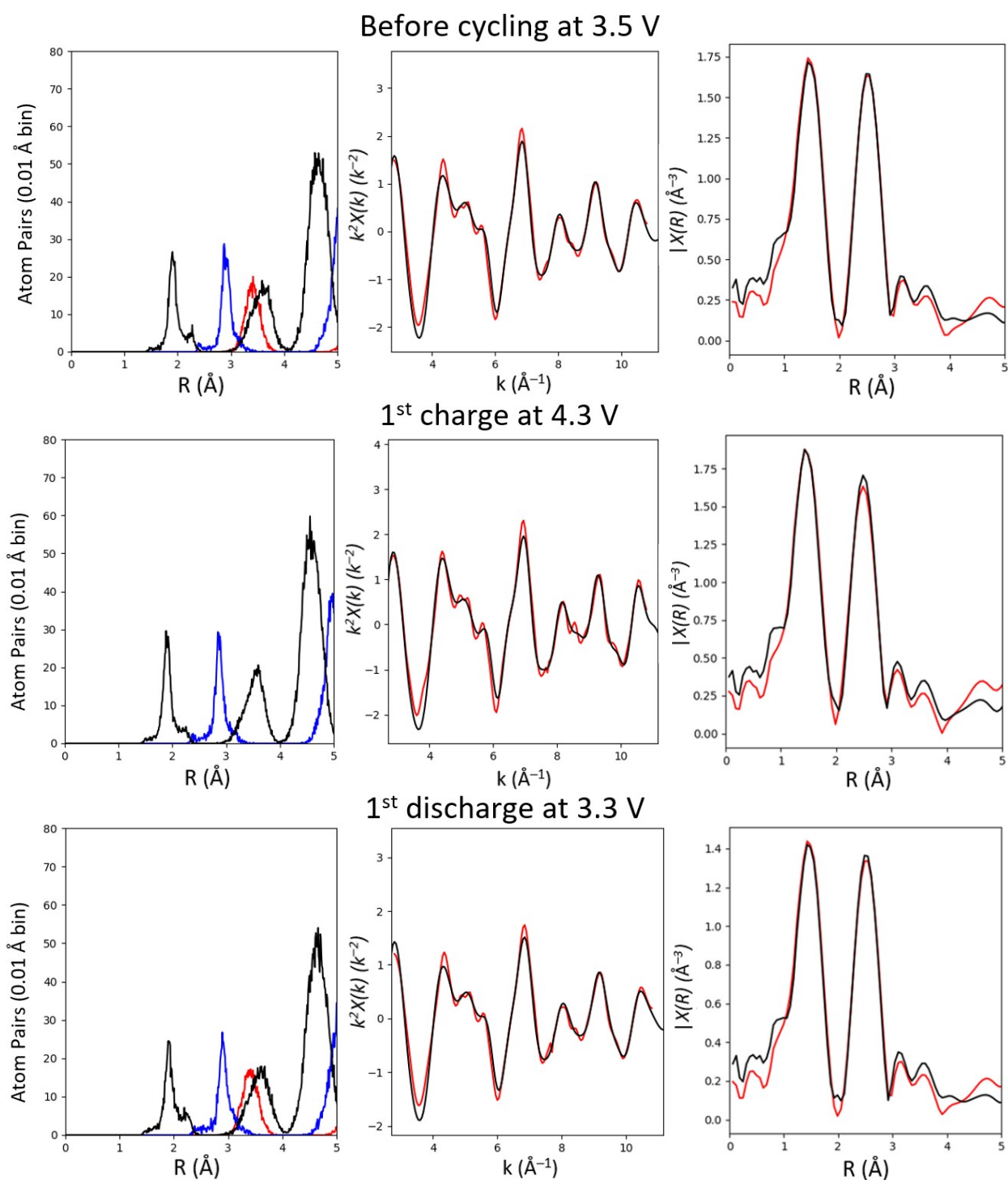


Figure S.3. Reverse Monte Carlo results of *operando* EXAFS data of nano-sized spinel collected before cycling at 3.5 V, 1st charge at 4.3 V and 1st discharge at 3.3 V.

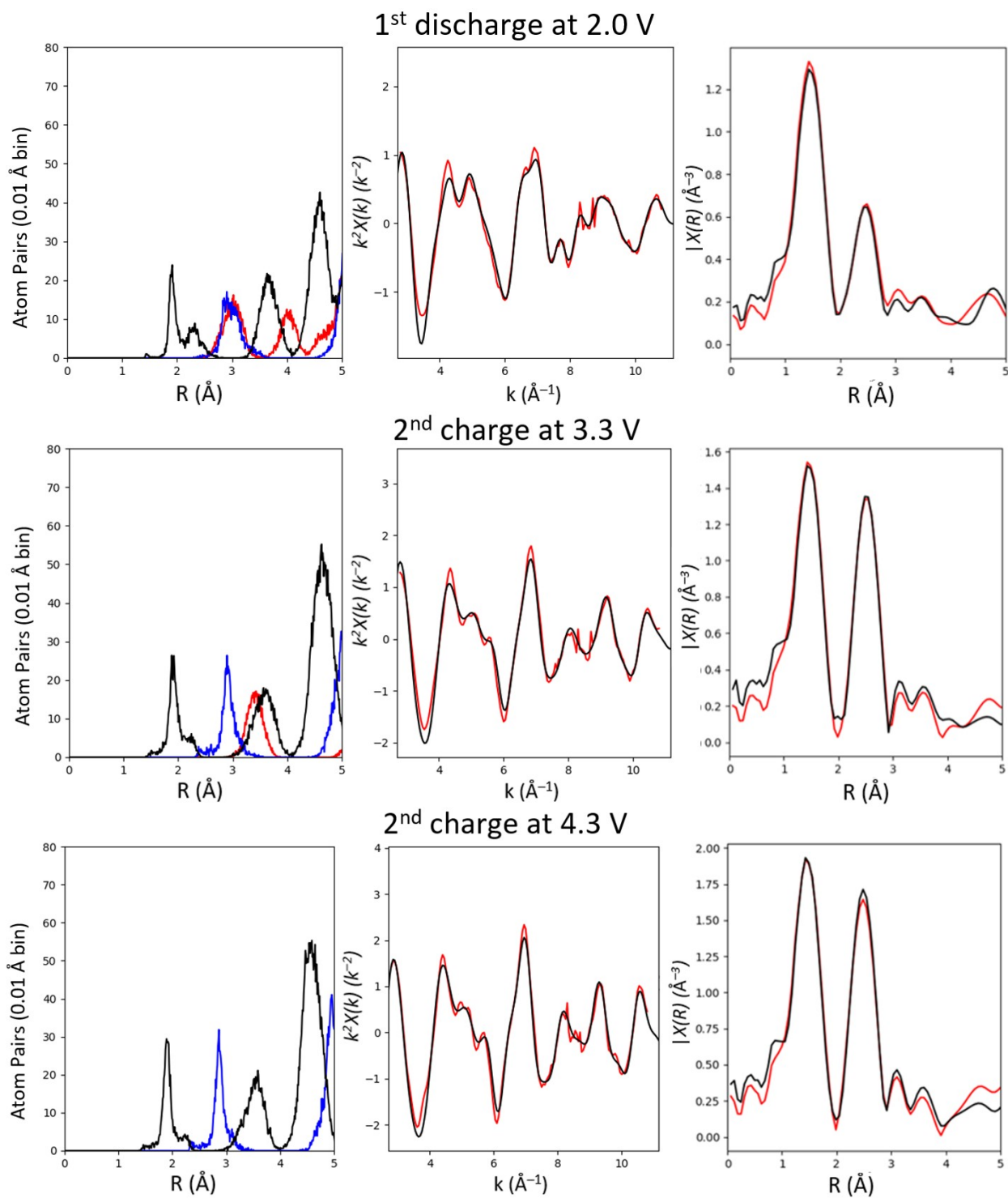


Figure S.4. Reverse Monte Carlo results of *operando* EXAFS data of nano-sized spinel collected 1st discharge at 2.0 V, 2nd charge at 3.3 V and 2nd charge at 4.3 V.

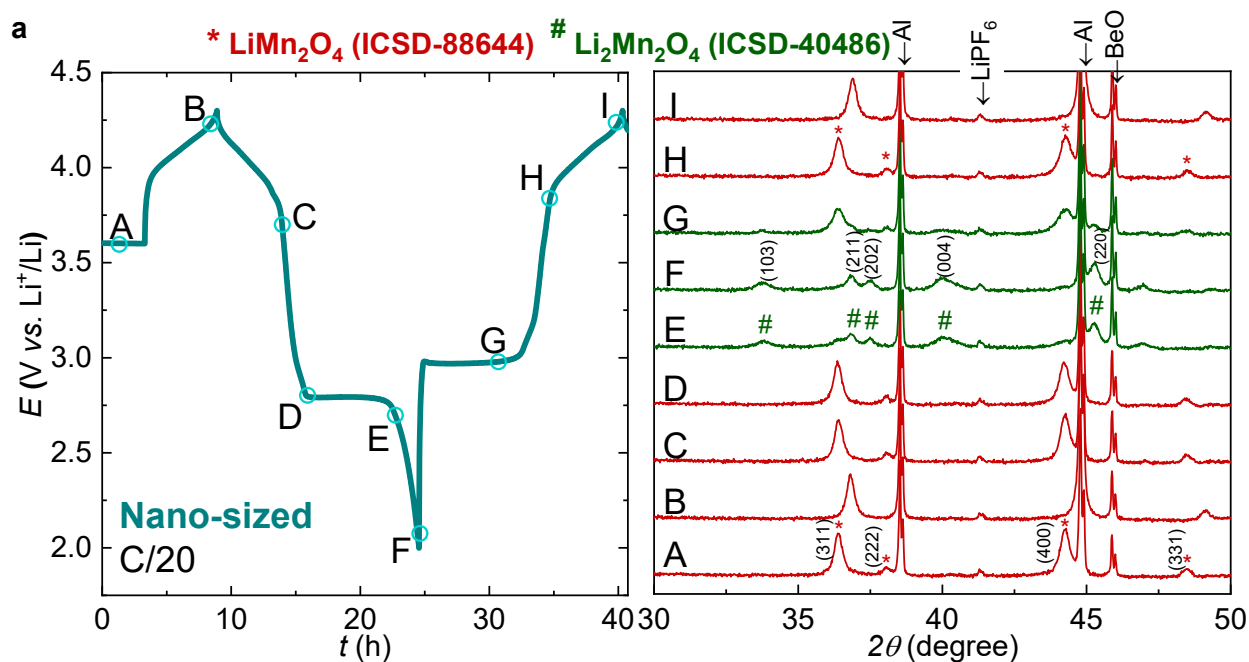


Figure S.5. Operando diffraction patterns (right panels) collected at different cycling (left panels) states to directly monitor the structural evolution of the nano-sized Li-rich $\text{Li}_x\text{Mn}_{2-x}\text{O}_4$ spinel cathode during one and a half cycles of charging to 4.3 V and deep discharging to 2.0 V at C/20 rate.

Comparison of FWHM of (311) reflection from main cubic phase in single-phase region of the nano-sized LMO cathode can be seen in the Figure 1. The difference between OCV and points during cycling comes from dynamic changes of crystal structure. However, the same cycling rate for the 1st and the 2nd charges and the same values of FWHM indicate lack of changes in crystallinity for this cathode material.

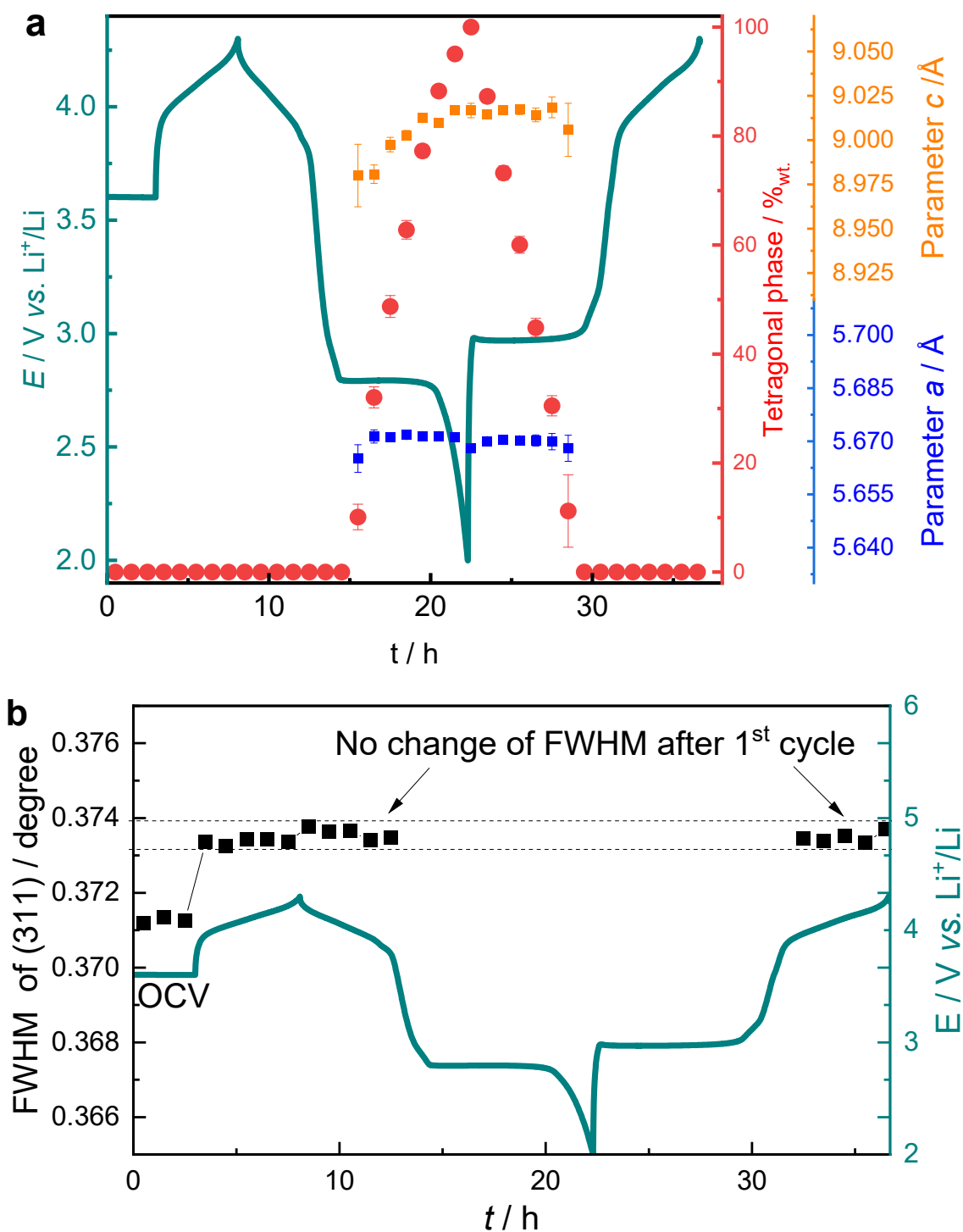


Figure S.6. Operando XRD analysis to track the evolution of different structures during the 1st cycle and the 2nd charge between 2.0 and 4.3 V of nano-sized Li-rich $\text{Li}_{1+x}\text{Mn}_{2-x}\text{O}_4$ spinel sample. (a) Galvanostatic charge/discharge profile of nano-sized spinel cathode (left axis, green) presented with corresponding results of Rietveld analysis of *operando* XRD patterns: amount of tetragonal phase (right axis, red) and $I41/amd$ lattice cell parameters a and c (right axis, blue and orange, respectively). (b) Galvanostatic charge/discharge profile (right axis, green) presented with the corresponding FWHM of (311) reflection from main cubic phase (left axis, black) calculated by Rietveld refinement of *operando* XRD patterns.

For the upper voltage range presented in the Table S.1 (data from *post mortem* XRD collected in the MS beamline at PSI and reported in our previously work Falqueto et al. (2022), the FWHM values of the reflections for the cubic spinel phase do not change comparing the as-synthesized with different cycling states (1st charge at 4.3 V, 1st discharge at 3.3 V, and after 200 cycles after discharge).

Table S.1. FWHM of the reflections for the nano-sized LMO spinel as-synthesized and at different cycling states between 3.3 and 4.3 V vs. Li⁺/Li at C/10 rate. The FWHM were extracted using the Pseudo-Voigt function in the fit analysis.

Reflection	As-synthesized		1 st charge at 4.3 V		1 st discharge at 3.3 V		200 cycles after discharge	
	FWHM / degree	Standard Error	FWHM / degree	Standard Error	FWHM / degree	Standard Error	FWHM / degree	Standard Error
(111)	0.06623	0.00017	0.06080	0.00010	0.06362	0.00015	0.06353	0.00013
(311)	0.09343	0.00050	0.07692	0.00025	0.08865	0.00040	0.08973	0.00037
(222)	0.07905	0.00227	0.07470	0.00120	0.07758	0.00173	0.07744	0.00168
(400)	0.11153	0.00050	0.08343	0.00020	0.10442	0.00041	0.10508	0.00038
(331)	0.10170	0.00214	0.08265	0.00099	0.09617	0.00167	0.09537	0.00157
(511)	0.12254	0.00141	0.09346	0.00060	0.11420	0.00116	0.11536	0.00109
(440)	0.11964	0.00074	0.09546	0.00035	0.10992	0.00060	0.11112	0.00056
(531)	0.12318	0.00208	0.09730	0.00082	0.11518	0.00156	0.11795	0.00152

Table S.2. Summary of Rietveld analysis results for the nano-sized Li-rich $\text{Li}_x\text{Mn}_{2-x}\text{O}_4$ spinel.

time / h	Rwp	Cubic phase, $Fd-3m$		Tetragonal phase, $I41/adm$		
		Amount / %wt.	parameter a / Å	amount / %wt.	parameter a / Å	parameter c / Å
0.5	3.6018	100	8.1947 (34)	0		
1.5	3.4955	100	8.1945 (33)	0		
2.5	3.6922	100	8.1951 (35)	0		
3.5	3.6277	100	8.1871 (34)	0		
4.5	3.8721	100	8.1685 (36)	0		
5.5	3.9582	100	8.1486 (38)	0		
6.5	3.9240	100	8.1277 (39)	0		
7.5	3.9930	100	8.1029 (40)	0		
8.5	3.9023	100	8.1080 (39)	0		
9.5	3.9966	100	8.1321 (39)	0		
10.5	3.7797	100	8.1546 (36)	0		
11.5	3.6883	100	8.1767 (35)	0		
12.5	3.6610	100	8.1930 (35)	0		
13.5	3.7561	100	8.1975 (35)	0		
14.5	3.8653	100	8.2002 (38)	0		
15.5	3.6610	89.9 (1.1)	8.2001 (43)	10.1 (2.4)	5.6651 (39)	8.9800 (176)
16.5	3.7278	68.0 (0.9)	8.2009 (53)	32.0 (1.9)	5.6714 (19)	8.9808 (52)
17.5	3.9456	51.3 (0.9)	8.1990 (68)	48.7 (2.0)	5.6711 (13)	8.9975 (41)
18.5	3.8729	37.2 (0.7)	8.1993 (87)	62.8 (1.7)	5.6718 (10)	9.0027 (28)
19.5	3.8731	22.7 (0.7)	8.2014 (132)	77.3 (1.2)	5.6715 (09)	9.0124 (20)
20.5	3.8007	11.8 (0.6)	8.2026 (240)	88.2 (0.6)	5.6715 (07)	9.0097 (17)
21.5	4.0041	4.9 (0.6)	8.2018 (571)	95.1 (0.7)	5.6712 (07)	9.0168 (15)
22.5	3.8729	0		100	5.6681 (10)	9.0167 (41)
23.5	3.8294	12.7 (0.6)	8.1986 (228)	87.3 (1.2)	5.6701 (07)	9.0146 (16)
24.5	3.8306	26.8 (0.7)	8.1960 (118)	73.2 (1.3)	5.6704 (09)	9.0169 (20)
25.5	3.9187	39.9 (0.8)	8.1962 (86)	60.1 (1.5)	5.6703 (12)	9.0172 (28)
26.5	3.9691	55.2 (0.9)	8.1966 (68)	44.8 (1.7)	5.6702 (16)	9.0142 (39)
27.5	4.0726	69.5 (1.0)	8.1964 (59)	30.5 (1.9)	5.6699 (23)	9.0185 (59)
28.5	4.0374	88.8 (2.7)	8.1966 (51)	11.2 (6.6)	5.6680 (37)	9.0058 (150)
29.5	4.1508	100	8.1970 (45)	0		
30.5	4.0341	100	8.1955 (42)	0		
31.5	3.9535	100	8.1912 (40)	0		
32.5	3.8205	100	8.1740 (38)	0		
33.5	3.8193	100	8.1551 (39)	0		
34.5	3.7814	100	8.1351 (41)	0		
35.5	3.7510	100	8.1127 (43)	0		
36.5	3.5802	100	8.0903 (40)	0		

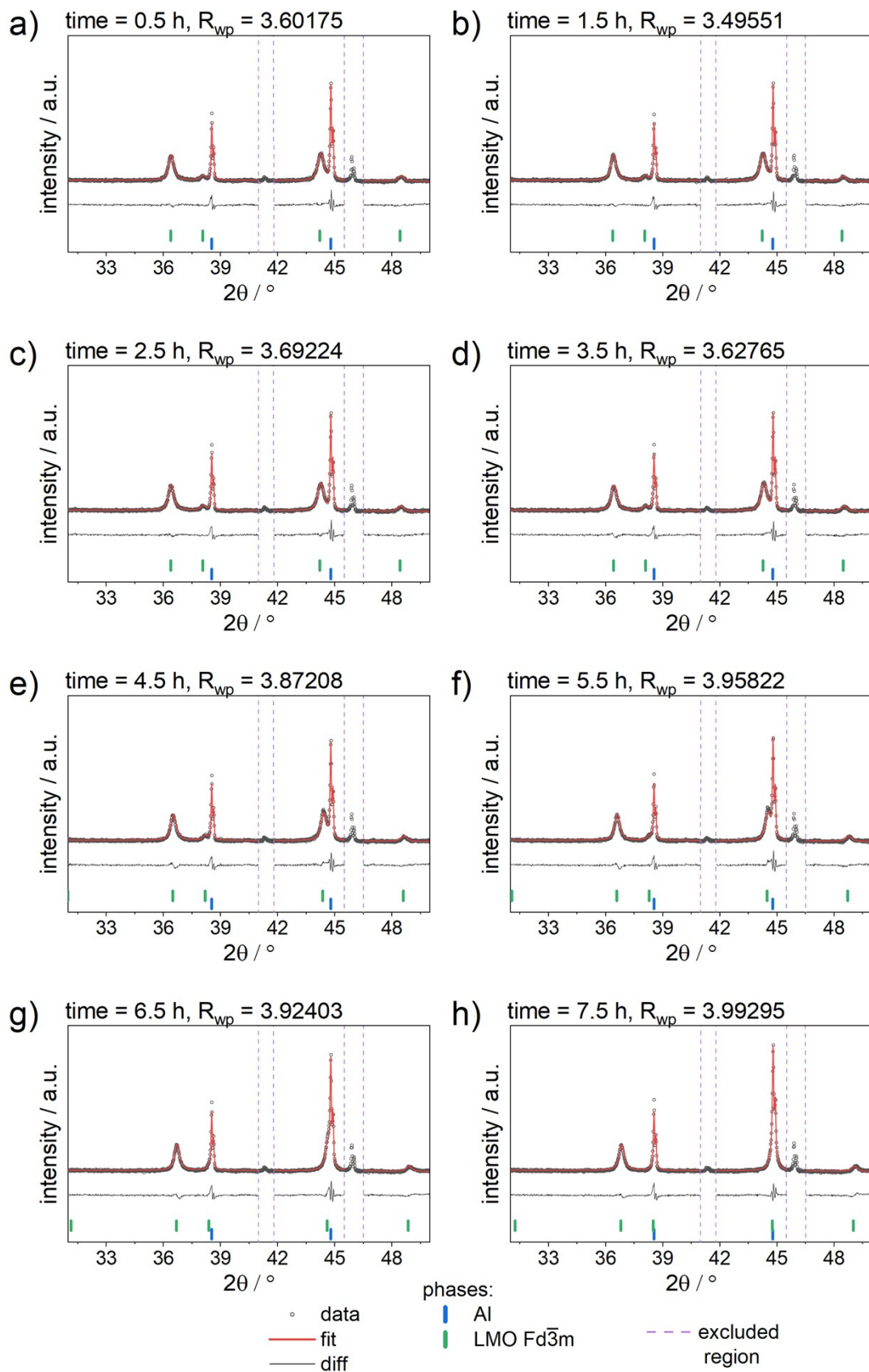


Figure S.7. Rietveld refinement results of *operando* XRD data of nano-sized spinel collected for scans 1 - 8 (a-h).

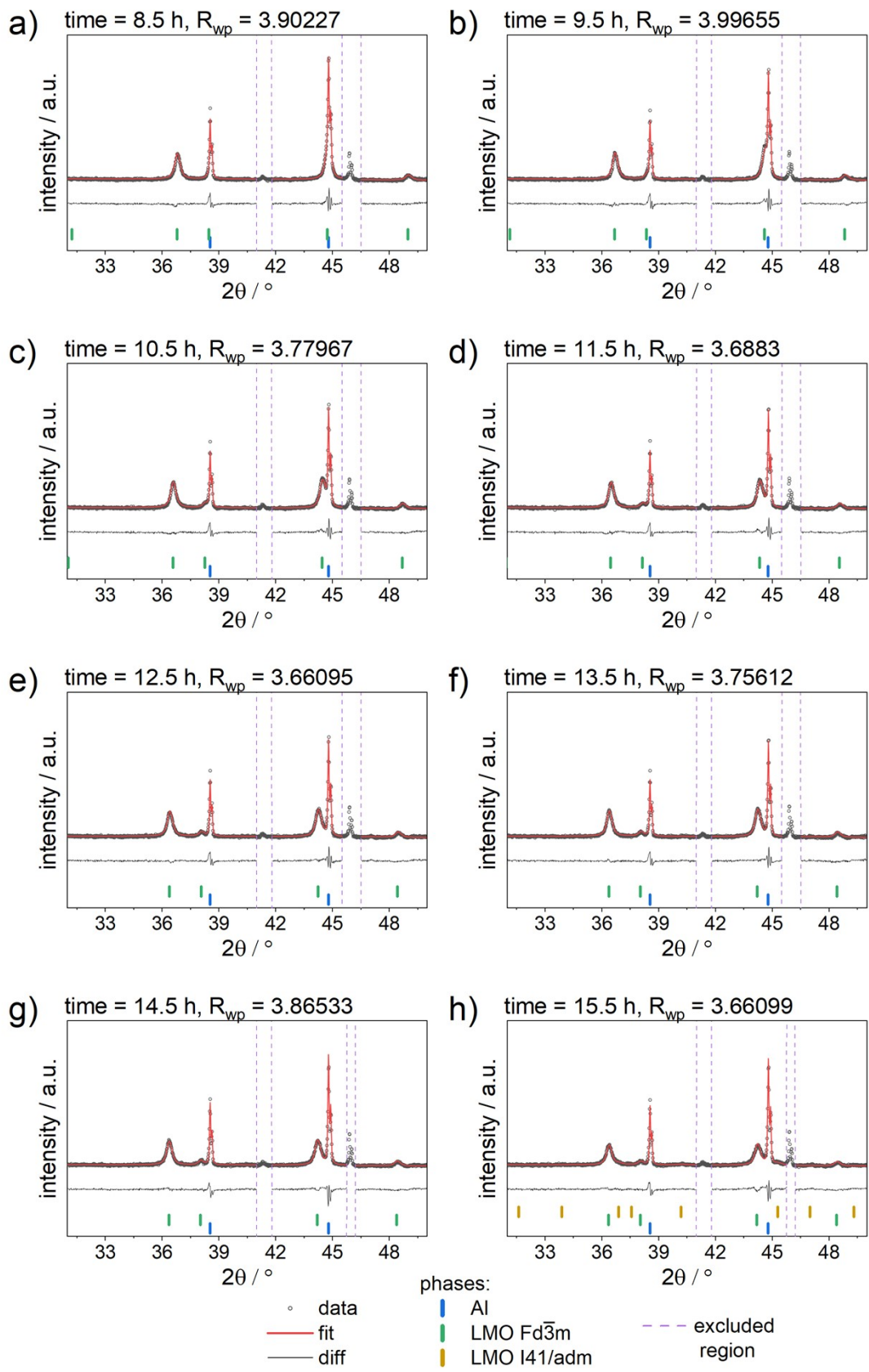


Figure S.8. Rietveld refinement results of *operando* XRD data of nano-sized spinel collected for scans 9 - 16 (a-h).

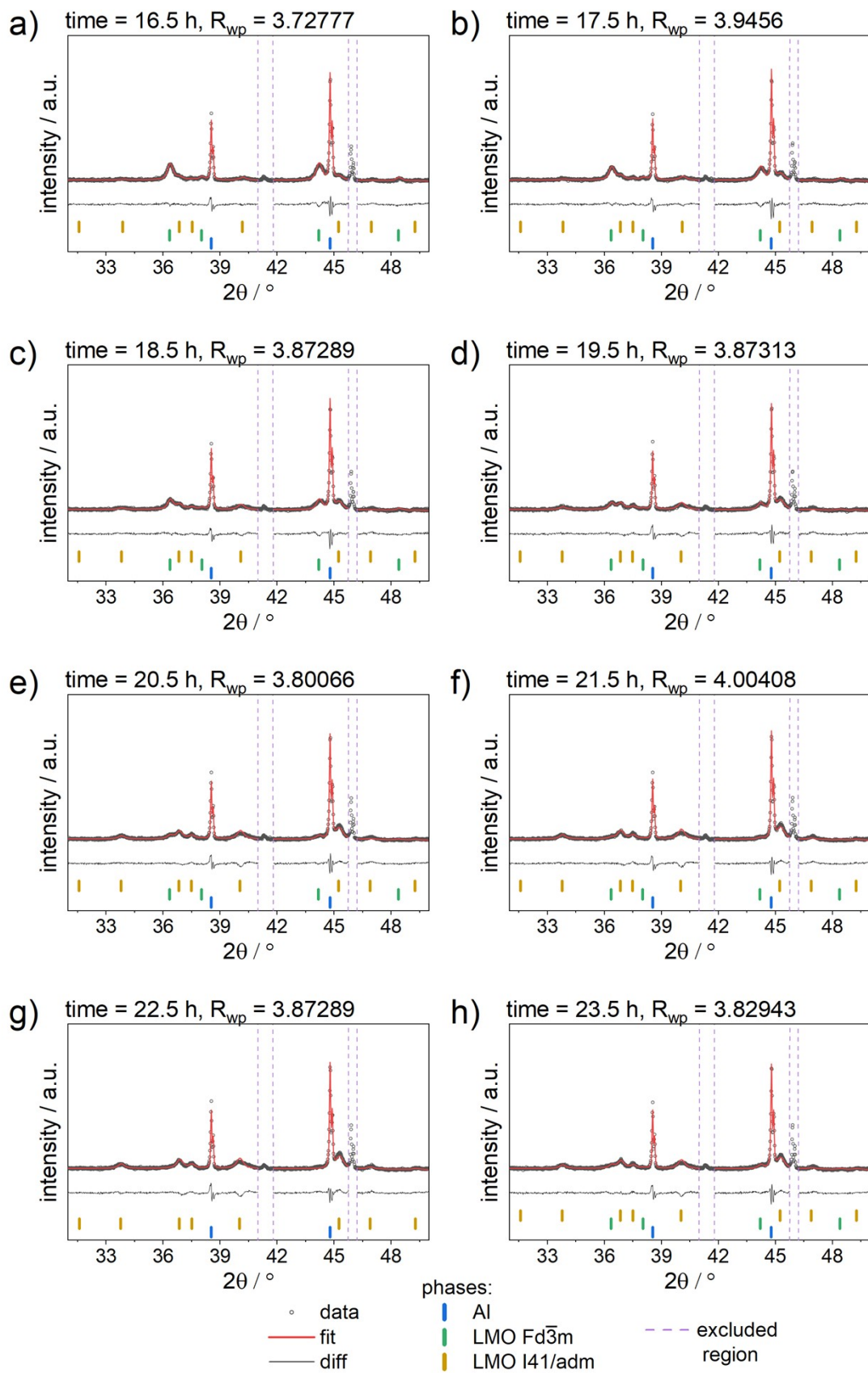


Figure S.9. Rietveld refinement results of *operando* XRD data of nano-sized spinel collected for scans 17 - 24 (a-h).

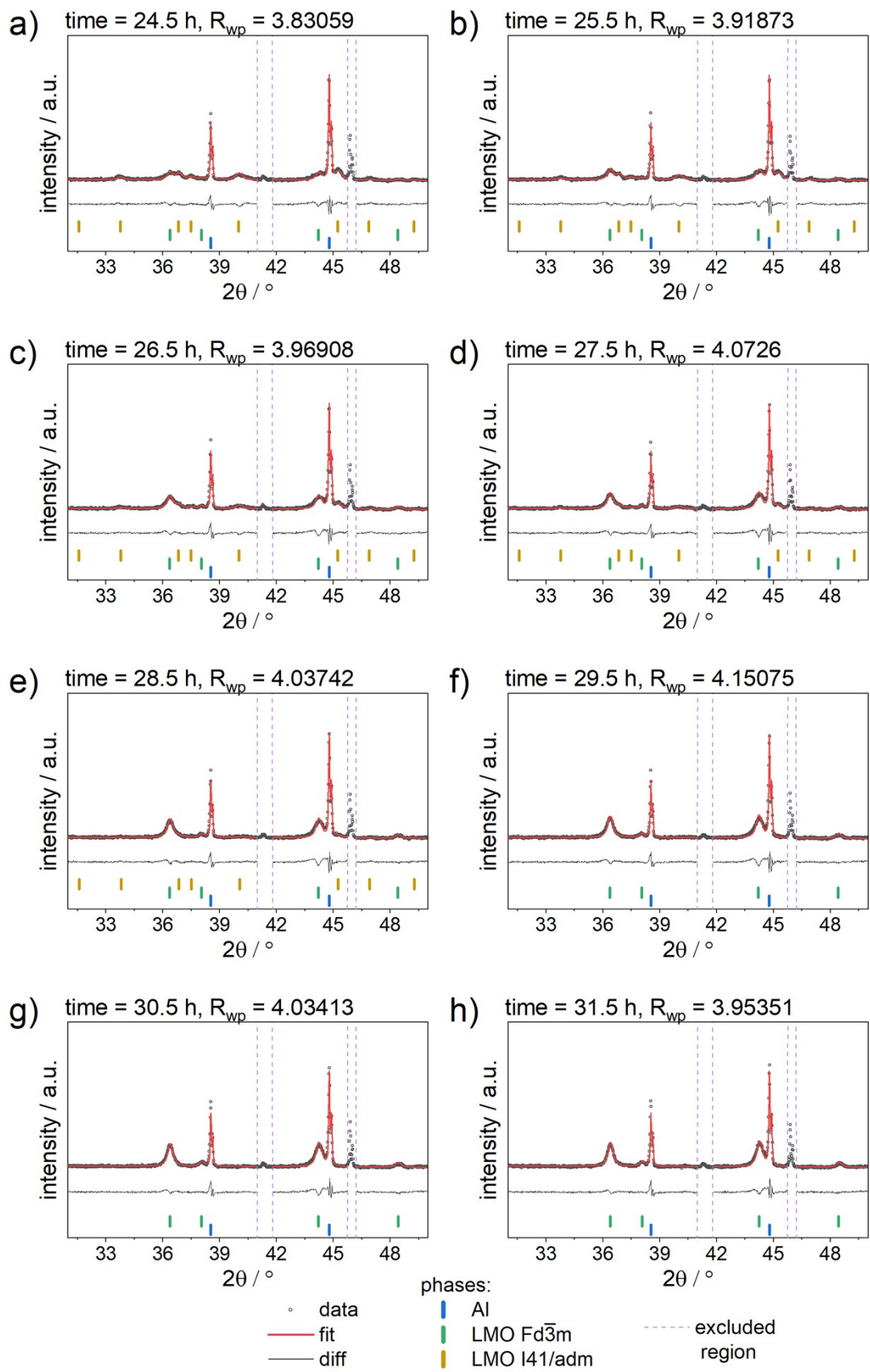


Figure S.10. Rietveld refinement results of *operando* XRD data of nano-sized spinel collected for scans 25 - 32 (a-h).

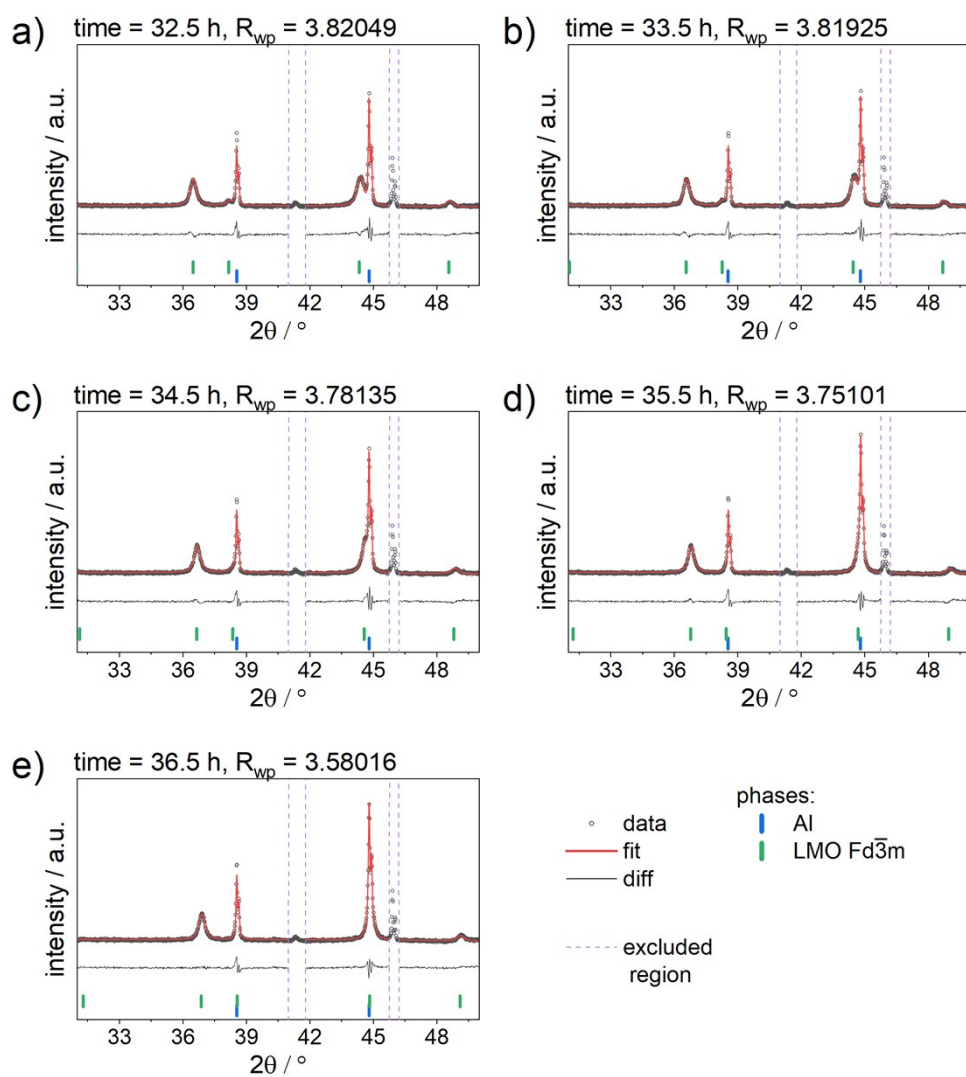


Figure S.11. Rietveld refinement results of *operando* XRD data of nano-sized spinel collected for scans 33 - 37 (a-e).

For the micron-sized spinel cathode (**Figure S.12**), it was observed that part of the active material is electronically inactive (~22%) due to some problems during the preparation of this electrode. Thus, the peak intensities presented in **Figure S.12b** were corrected by subtracting the diffraction pattern collected before cycling at OCP (used as a reference) from the subsequent diffraction patterns collected during cycling. The contour plot with the diffraction patterns before correcting for intensities is presented in **Figure S.12a**.

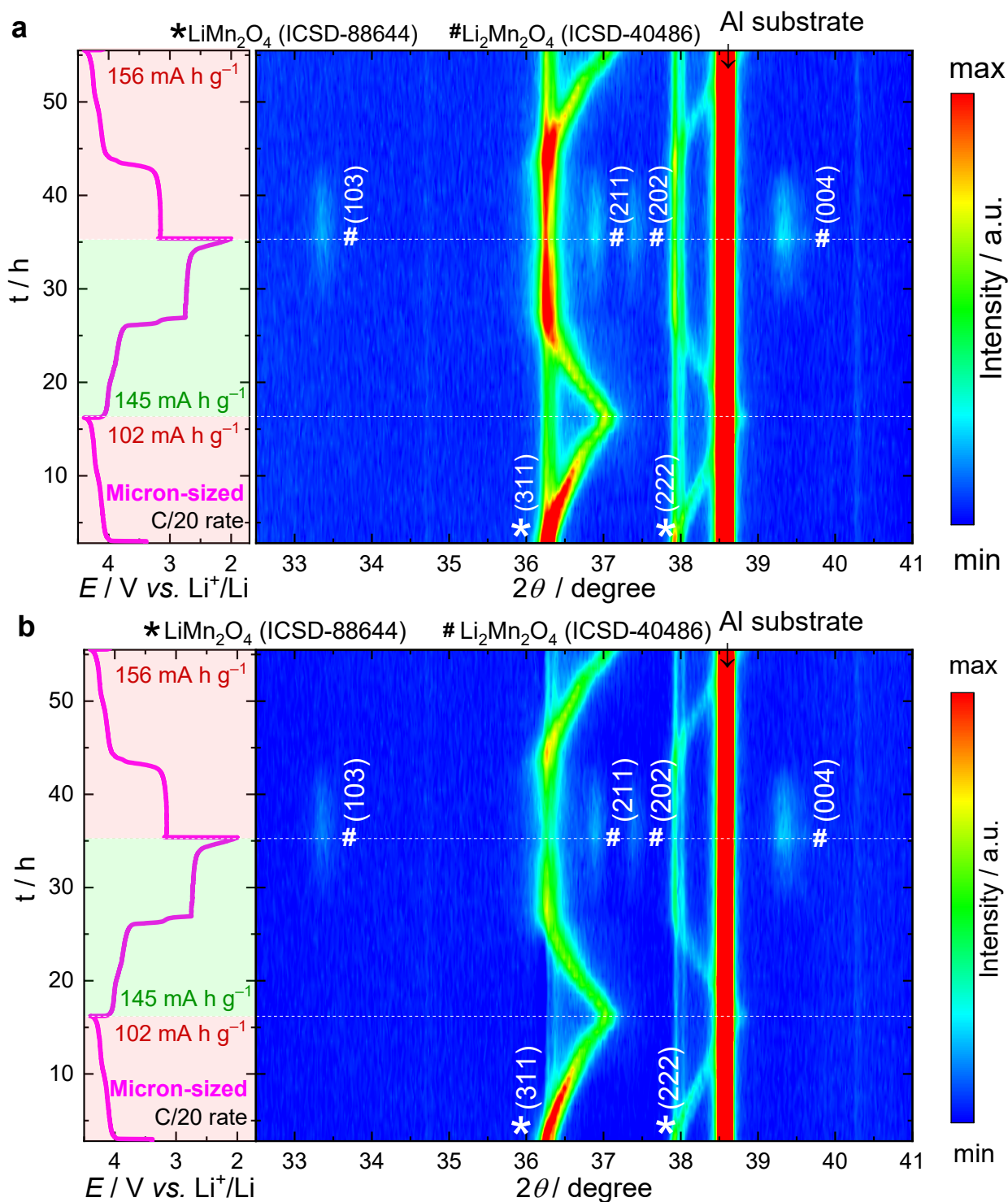


Figure S.12. *Operando* XRD analyses to track the evolution of different structures during 1st cycle and 2nd charge of electrode prepared from micron-sized LiMn_2O_4 spinel (a) before and (b) after correction the patterns intensity.

For the nano-sized electrode, two distinct peaks rise with the increasing of cycle number, while for the micron-sized, the two peaks already appear in the first cycle (**Figure S.13**). Additionally, it was observed changes in the peak positions among the dQ/dV curves for the nano-sized, confirming the changes on the energy level of the tetrahedral sites for Li^+ deintercalation/intercalation. It is good to mention here that it was observed only the tetrahedral phase in the diffraction patterns collected in this voltage range (**Figure 4**). No detectable change in the peak position among the dQ/dV curves was observed for the micron-sized cathode.

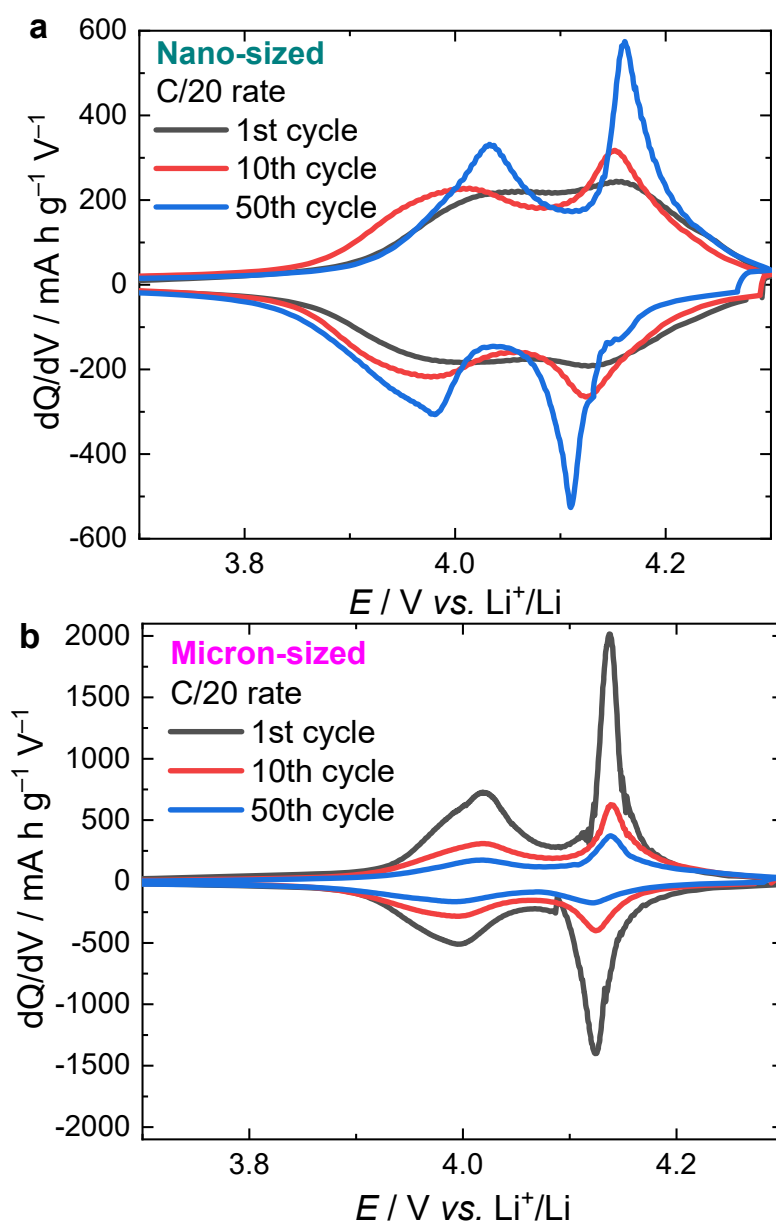


Figure S.13. dQ/dV curves obtained from 1st, 10th, and 50th cycle at C/20 rate presented in the **Figure 5c**, for (a) nano-sized and (b) micron-sized spinel cathodes.

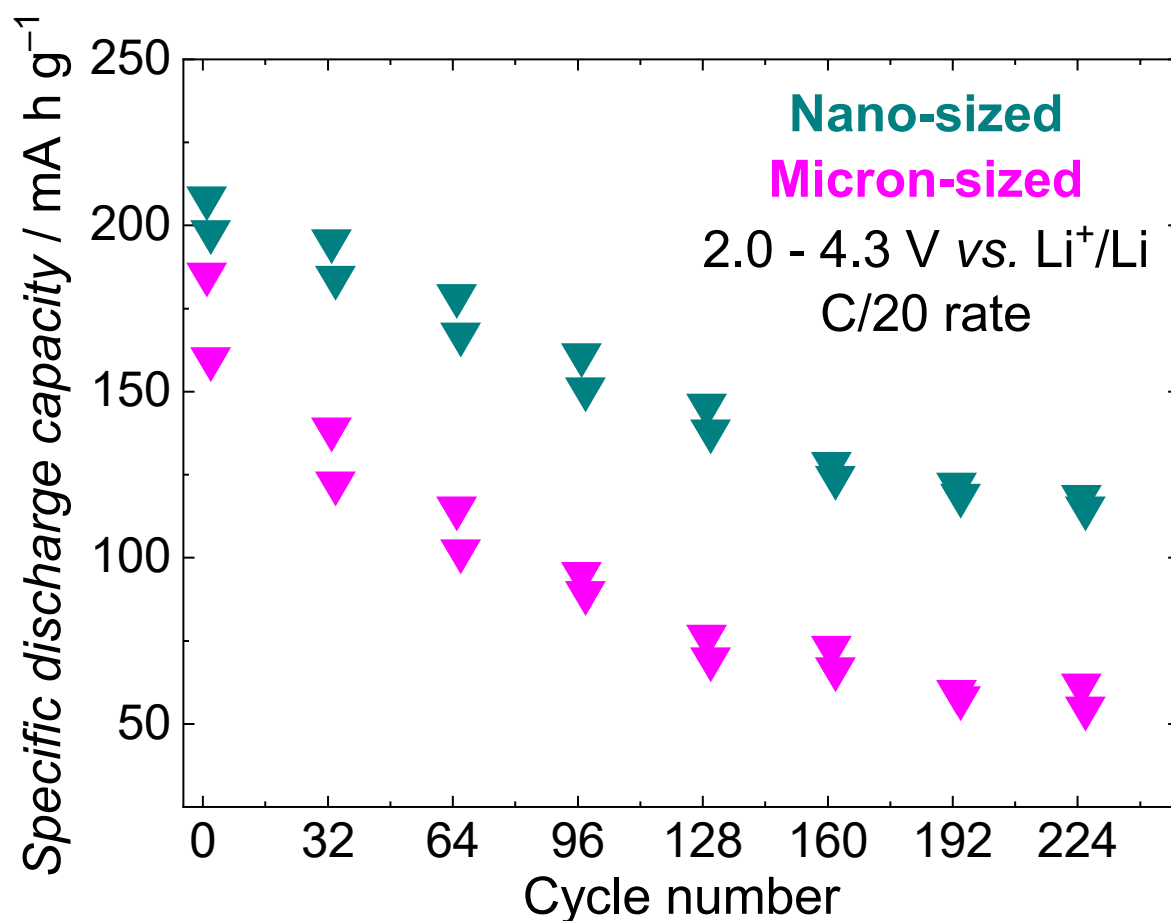


Figure S.14. Specific discharge capacity obtained for the nano and micron-sized spinel cathodes cycled in a voltage range of 2.0 – 4.3 V at C/20 rate using the cycling protocol presented. Both cathodes present a decay of the initial values of specific discharge capacity as the cycle number increases, being less pronounced for the cathode prepared from nano-sized than that from micron-sized spinel.

References

Falqueto, J. B., Clark, A. H., Štefančič, A., Smales, G. J., Vaz, C. A. F., Schuler, A. J., Bocchi, N., & El Kazzi, M. (2022). High Performance Doped Li-Rich $\text{Li}_{1+x}\text{Mn}_{2-x}\text{O}_4$ Cathodes Nanoparticles Synthesized by Facile, Fast, and Efficient Microwave-Assisted Hydrothermal Route. *ACS Applied Energy Materials*, 5(7), 8357–8370. <https://doi.org/10.1021/acsaem.2c00902>